nature neuroscience

Persistent neural activity in the human frontal cortex when maintaining space that is off the map

Kyeong-Jin Tark[1] & Clayton E Curtis[1,2]

During the maintenance of visuospatial information, neural activity in the frontal eye field (FEF) persists and is thought to be an important neural mechanism for visual working memory. We used functional magnetic resonance imaging to examine whether human FEF activity persists when maintaining auditory space and whether it is selective for retinal versus extra-retinal space. Subjects performed an audiospatial working-memory task using sounds recorded from microphones placed in each subject's ear canals, which preserved the interaural time and level differences that are critical for sound localization. Putative FEF activity persisted when maintaining auditory-cued space, even for locations behind the head to which it is impossible to make saccades. Therefore, human FEF activity represents both retinal and extra-retinal space.

The short-term storage of the locations of information in our environments with respect to our body endows us with greater flexibility in the planning and execution of our actions, as they are not continually dependent on visual guidance. The prefrontal cortex (PFC), which sits at the apex of the motor hierarchy, is believed to be critical for the maintenance of space. First, lesions of the dorsal lateral PFC (dlPFC) and FEF cause impairments in spatial working memory, as indexed by the accuracy of a saccade made to the location of a past visual cue[1–5]. Second, dlPFC and FEF neural activity persists during the maintenance of spatial positions in working memory[6–10]. Persistent neural activity is thought to be the mechanism that temporally bridges the past sensory cue and its later and contingent memory–guided action[11]. Persistent activity carries information about the location of past sensory events or the direction of forthcoming motor plans. Specifically, a population of visual cells with varying visual receptive fields could maintain locations in retinotopic coordinates. Similarly, a population of saccade cells with varying motor response vectors could maintain locations through persistent activity, but their activity would represent the prospective coding of the future memory–guided saccade.

Both of these neural mechanisms imply that space is coded by the dlPFC and FEF in retinal coordinates and eye-centered reference frame. We asked what happens to these persistent activations when we maintain spatial positions off the retinal map (that is, locations behind the head to which there are no retinal representations and to which saccades cannot be made). To do so, we measured brain activity while subjects maintained working-memory representations of auditory-cued spatial locations, half of which were perceived to be emanating from behind their head (**Fig. 1a**,**b**). We tested two main hypotheses about the involvement of the frontal cortices in spatial working memory. We first tested whether activity in the dlPFC persists while the subjects maintained auditory-cued spatial locations that were in retinal space (that is, locations that would fall on the retina if they were visual and not auditory). We then tested whether dlPFC activity would persist when maintaining spatial locations behind the head, beyond retinal space. We predicted that activity in the dlPFC, including the putative human FEF, would only persist when maintaining locations in retinal space, as it is thought that the monkey FEF is composed of neurons with retinal or eye-centered representations of space. To our surprise, activity persisted even when subjects maintained space behind their heads, that is, off the retinal map.

RESULTS

To test these hypotheses, we carried out an auditory spatial working-memory task that required subjects to maintain an auditory cued location over a retention interval and then decide whether the following probe location matched or not. We then compared the results of this task with those obtained during the generation of saccades and the maintenance of visually cued space.

Behavioral results

By design, the staircase procedures equated the accuracy for the front and back auditory spatial working memory trials (**Fig. 1**). Performance improved predictably as the distance between the location of the sample and test sound increased. Using this relationship, we kept the performance accuracy for front and back space trials at the target threshold of 75% for each subject (**Fig. 1c**). We created psychometric functions[12] for the front and back space trials separately, and examined the relationship between the distance between the sample and test sound locations and performance accuracy (**Fig. 1d**). Because task performance was equated, we were able to compare blood oxygen level–dependent (BOLD) responses during front and back trials. In addition, as performance did not change as a function of the delay period lengths that we used (**Supplementary Fig. 1**), we collapsed the data across the delay lengths in our statistical analyses.

[1]Department of Psychology, [2]Center for Neural Science, New York University, New York, New York, USA. Correspondence should be addressed to C.E.C. (clayton.curtis@nyu.edu).

Received 7 July; accepted 28 August; published online 4 October 2009; doi:10.1038/nn.2406

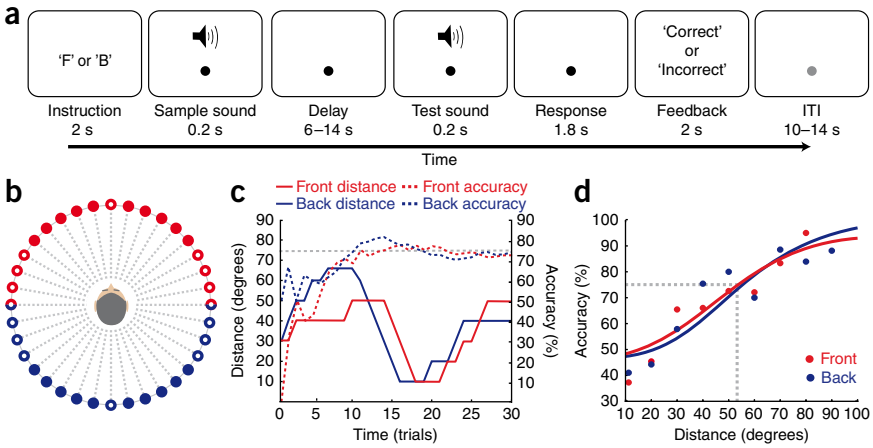

Figure 1 Task design and behavioral data. (**a**) Auditory spatial working-memory task schematic. Each trial began with an instruction foretelling a front ('F') or back ('B') space trial. Subjects maintained the location of a sample sound over a delay period and then indicated whether the location of the test sound matched the sample sound. (**b**) Spatial positions of sound recordings made at 10° increments around the subject's head. Red and blue indicate front and back space, respectively. The unfilled dots are positions where the sample sound never occurred because of the difficulties discerning front or back and left or right. (**c**) Behavioral data from a representative subject. The solid lines depict the distance of the test sound from the sample sound on nonmatching trials. The dashed lines depict the running accuracy of performance. Performance on front and back trials was effectively maintained at 75% accuracy by staircases that adjusted the distance between the sample and test sounds. (**d**) Psychometric functions for the group across all sessions depict the relationship between performance accuracy and the distance between the sample and test sound locations. Dots indicate empirical data and lines indicate the fits to the data. As the distance between the sample and test sound locations increased, accuracy increased. However, there were no differences in overall performance of front and back trials. As a result of the staircase, subjects were, on average, 72% accurate on both front and back trials. The mean (± s.e.m.) response times were 912 ± 32 ms and 941 ± 24 ms on front and back trials, respectively. ITI, intertrial interval.

Surface-based statistical tests

We quantitatively evaluated the cortical activations evoked by processing the audiospatial cue and maintaining spatial locations (**Fig. 2**). During the cue period, when subjects encoded the location of a sample sound, we found robust activations in the superior precentral suclus (sPCS), posterior portions of the superior temporal gyrus (sTG), the inferior parietal lobule (iPL) bilaterally and the left inferior frontal sulcus. During the maintenance epoch, strong activations were elicited in sPCS and a posterior portion of sTG bilaterally. Compared with activation in the right hemisphere, additional activations in the left central sulcus and left postcentral area were observed during the delay period, which probably resulted because subjects were holding a button box and preparing to make button presses with their right hand.

We also contrasted the activations of the front and back condition to examine whether there are brain regions that are specialized for maintaining retinal versus extra-retinal space. During the delay period, there were no significant differences ($P > 0.05$).

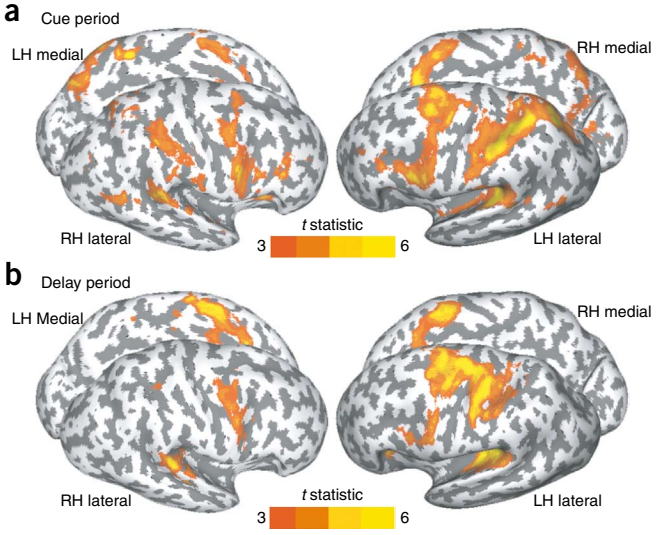

Figure 2 Surface-based statistical maps. (**a**,**b**) Significant activations are overlaid on cortical surface rendering where dark gray color indicates sulcal and light gray color indicates gyral areas. Note the activation in the sPCS, iPL and sTG bilaterally. LH, left hemisphere; RH, right hemisphere.

Region of interest (ROI) time-series analysis

Next, we plotted the time series in several ROIs to further test our hypotheses. Because we found no differences between the right and the left hemispheres, we collapsed data across the hemispheres. First, we asked whether activity would persist during the retention of auditory-cued spatial locations. We determined the mean BOLD response in each ROI, time-locked to the presentation of a sample sound (**Fig. 3**). The sample sound evoked a transient response in each ROI. Following this transient response, BOLD activity persisted above baseline throughout the retention interval in sPCS (front, $t_{12} = 4.30$, $P < 0.01$; back, $t_{12} = 2.75$, $P < 0.03$) and iPL (front, $t_{12} = 4.14$, $P < 0.01$; back, $t_{12} = 1.92$, $P > 0.05$). Although the sTG was active during the delay, the activity was not sustained throughout the delay period (front, $t_{12} = -1.22$, $P > 0.05$; back, $t_{12} = 0.58$, not significant). To further confirm that the sPCS activity did indeed persist throughout the entire retention interval, we plotted the BOLD responses for each delay length (**Fig. 4**). sPCS activity clearly persisted above baseline even at the longest delay of 14 s and it did so when maintaining space in front and behind the head.

Second, we examined whether each hemisphere would show greater activation when maintaining positions in contralateral space than in ipsilateral space. In contralateral and ipsilateral trials, the delay period activity showed a contralateral bias in the sPCS and iPL for front space (**Fig. 3**). Only the sPCS showed greater contralateral activation during maintenance of back space. To quantify laterality biases, we computed a laterality bias index for the cue and delay periods in each ROI (**Fig. 5**, see Online Methods). The sPCS showed a significantly greater response to contralateral sounds and the maintenance of contralateral space for front and back space trials (cue front, $t_{12} = 2.70$, $P < 0.01$; delay front, $t_{12} = 2.23$, $P < 0.05$; cue back, $t_{12} = 2.15$, $P < 0.05$; delay back, $t_{12} = 2.71$, $P < 0.01$; **Fig. 5**). In the iPL, a bias was only found during the delay period for contralateral front, but not back, space (cue front, $t_{12} = -0.19$, $P > 0.05$; delay front, $t_{12} = 3.62$, $P < 0.01$).

Third, we tested for potential differences in activity when maintaining front and back spatial locations. Only one of these comparisons

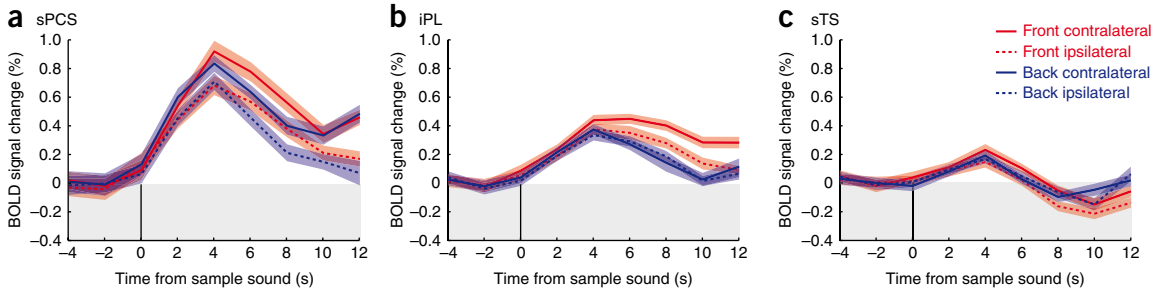

Figure 3 Group-averaged BOLD time courses time locked to the presentation of the sample sound in the three ROIs. (**a**) The sPCS activity persisted throughout the delay period when maintaining a location in front and back of the head. The activity was also significantly higher when maintaining contralateral compared with ipsilateral locations. (**b**) The iPL activity only persisted when maintaining locations in front of the head. (**c**) Activity in sTS only showed a brief transient response time locked to the sample sound. Error bands indicate average standard error across subjects.

reached statistical significance. During the delay period, activity was greater for front than back trials in the iPL ($t_{12} = 2.43$, $P < 0.05$). In other comparisons, the activity during front and back trials did not differ significantly ($P > 0.3$). In general, the iPL only showed strong delay-period activity for front contralateral trials, suggesting that it may only be involved in the maintenance of contralateral retinal space. It was surprising to us that the BOLD activity in sPCS, the putative human FEF, was not different during the maintenance of front versus back space. However, consistent with these results, a multivoxel pattern analysis of the BOLD response in sPCS could not reliably distinguish between front and back space (see **Supplementary Results 1** and **Supplementary Fig. 2**).

Saccade generation and visual spatial working memory

A subset of the subjects ($n = 5$) were recruited for a follow-up scanning session in which we measured BOLD activity while subjects performed a saccade-localizer task (see Online Methods). The saccade and the auditory spatial working-memory tasks evoked overlapping patterns of activity in the sPCS (**Fig. 6a**). Therefore, the same part of the sPCS that was involved in saccade generation was also involved in the maintenance of auditory-cued space.

We then asked whether the same part of the sPCS is active during the maintenance of visual- and auditory-cued space. The visual and auditory spatial working-memory tasks were almost identical except for the difference in sensory modality. Notably, delay period–specific activity during the auditory and visual working-memory tasks evoked overlapping patterns of activity in the sPCS (**Fig. 6b**).

In fact, the overlapping pattern of sPCS activation can be seen at the single-subject level. We plotted the delay-period activation for the auditory and visual spatial working-memory tasks in each of the five subjects (**Fig. 7**).

Finally, we defined a putative human FEF ROI on the basis of voxels in the sPCS that were significantly active during the saccade localizer task in each of the five subjects. We plotted the time courses from these ROIs to test whether BOLD activity would persist during the retention of auditory-cued space, as we demonstrated above in the full sample using ROIs not defined by saccade execution. Using the exact same ROI, we tested whether BOLD activity persisted during the retention of visual-cued spatial locations, as we have found in past studies[13–15]. Indeed, following a transient response in sPCS time-locked to the presentation of both an auditory and visual spatial cue, BOLD signals persisted above baseline throughout the retention interval (**Fig. 8**). The same

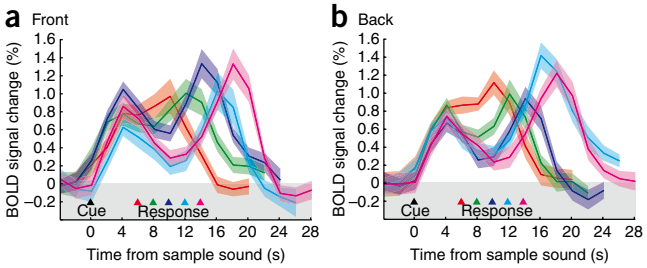

Figure 4 Group-averaged BOLD time courses time locked to the presentation of the sample sound in the sPCS. (**a**,**b**) Group-averaged BOLD time courses time locked to the presentation of the sample sound in the sPCS. Each line represents data from a different delay length where the beginning of the delay is marked with the black triangle and the ends of the delay are marked by the colored triangles. Book-ended by transient responses time locked to the sample and test sounds, delay-period activity remained above baseline even at the longest delay of 14 s (pink line).

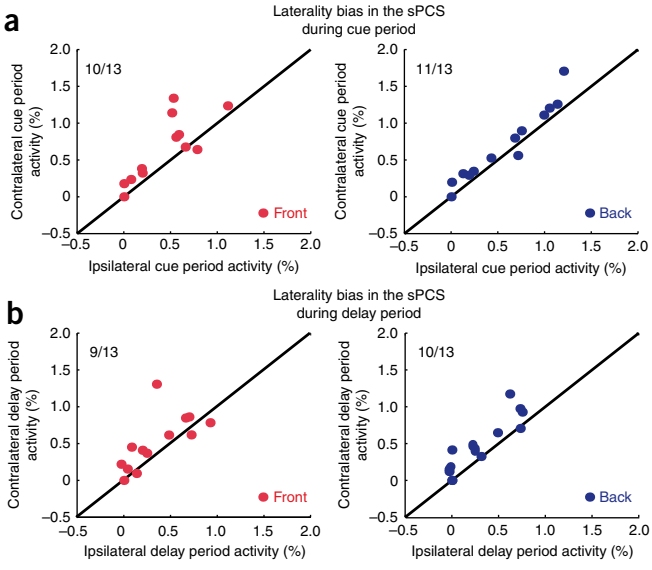

Figure 5 Scatter plots quantifying the laterality bias in the sPCS. (**a**,**b**) Almost all of the subjects showed greater activity in the sPCS hemisphere contralateral to the location of the sample sound compared with the ipsilateral sPCS activity. The red and blue dots depict each subject's level of BOLD activity during the front and back space trials, respectively. The ratio given in the top left is the number of subjects whose activity showed a contralaterality bias (that is, fell above the line of equality).

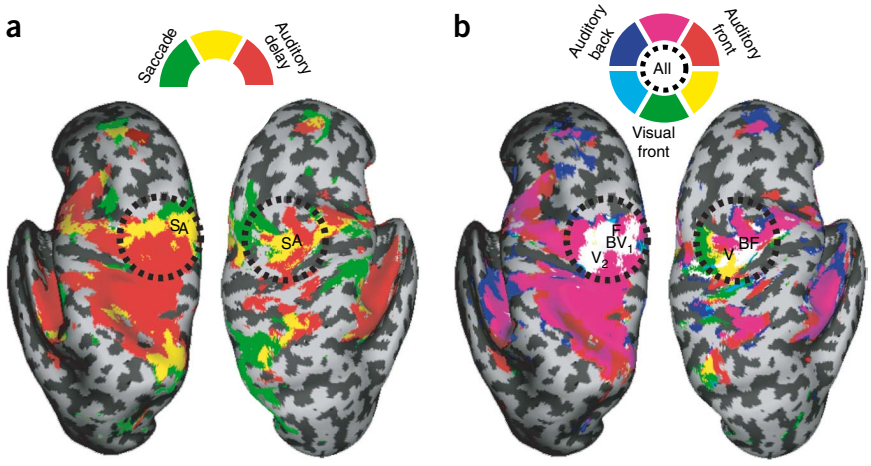

Figure 6 Group comparisons of auditory spatial working memory with saccade generation and visual spatial working memory. For comparison purposes, five subjects in the study were also scanned while making visually guided saccades and during a visual spatial working-memory task. (**a**) We compared significant delay-period activity (see Online Methods) during the auditory spatial working-memory task (colored red) with activity evoked by saccade generation (colored green). Note the extensive overlapping activity in the sPCS (colored yellow). The letters mark the peaks of the *t* maps for saccade related (S) and auditory spatial working-memory delay-period activity (A). (**b**) We compared the delay-period activation during the auditory with a similar visual working-memory task. The colors represent significant activity during the delay period of the auditory spatial working memory task during front (red color) and back (blue color) trials and the delay period activity during the visual spatial working-memory task (green color). The letters mark the peaks of the *t* maps for delay-period activity during the auditory front (F), auditory back (B) and visual (V) spatial working-memory trials. V_1 and V_2 denote the two peaks that emerged in the left hemisphere. Note the extensive overlapping activity in the sPCS (colored white). The Montreal Neurological Institute coordinates are given in **Supplementary Tables 1** and **2** and are consistent with the location of the putative human FEF[36–38].

tissue in the sPCS persisted during the maintenance of auditory and visual cued space, even when the space that was being remembered was extra-retinal or behind the head.

DISCUSSION

We confirmed our hypothesis that BOLD activity in the sPCS, the putative human homolog of the monkey FEF, persists when maintaining the locations of auditory cues, similar to when maintaining visual-cued space[13,14,16]. Although this finding is not surprising, as electrophysiological recordings from monkey FEF neurons show persistent activity during auditory spatial working memory delays[17–19], it does provide an important translational link to animal models of human spatial cognition.

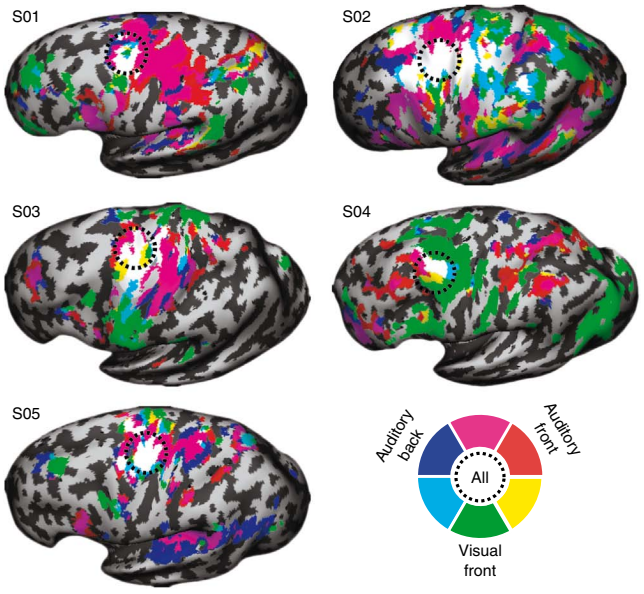

Figure 7 Individual subject comparisons of auditory- and visual-cued spatial-working memory. Each of the five subjects' left hemispheres are shown with the same nomenclature as in **Figure 6b**.

Notably, we were able to reject the hypothesis that the putative human FEF only persists when maintaining retinal space to which saccades can be made. BOLD activity in the human FEF persisted when maintaining spatial locations behind the head. These results are notable because activity persisted even when maintaining spatial locations to which an eye movement cannot be made, a finding that current theories are at odds with or at least agnostic about. Traditionally, the FEF is thought to represent space in retinal- or eye-centered coordinates; visual FEF neurons have spatially selective receptive fields and motor FEF neurons have response fields, both of which are in retinal coordinates[20–23]. However, our data suggest that the human FEF contains at least some neurons whose activity represents extra-retinal space, possibly in head- or body-centered coordinates.

We draw this conclusion for several reasons. First and foremost, BOLD signal in the FEF persisted during the delay period when subjects were maintaining space behind the head. It would be inefficient, at best, if a retinotopic brain area that is purported to control eye movements contains neurons that represent space beyond the retina or off the oculomotor map. Second, we found a contralateral bias in FEF activity when subjects maintained extra-retinal space. This is important because it rules out the possibility that the persistent activity could be caused by non-mnemonic factors, such as active fixation or increases in general attention. Third, the persistent activity is unlikely to be related to eye movements or eye-movement planning. Subjects were not required to make eye movements during the auditory spatial working-memory task, fixation was monitored with an eye tracker, and trials in which subjects made uninstructed eye-movements were excluded from our analyses. Other data also suggest the FEF may contain neurons that code for extra-retinal space. For example, electrical stimulation of FEF neurons induces not only eye movements, but also sometimes induces head movements[24–26]. Moreover, FEF microstimulation evokes neck muscle activity associated with coordinated eye-head gaze shifts even when the eye movement is small and not accompanied by a head movement[27]. These findings suggest that the FEF contains spatial representations that are used to control the orientation of gaze. Indeed, congenitally blind individuals who tend to orient to space with head instead of eye movements show FEF activation during shifts of covert attention[27]. Together, these findings suggest that

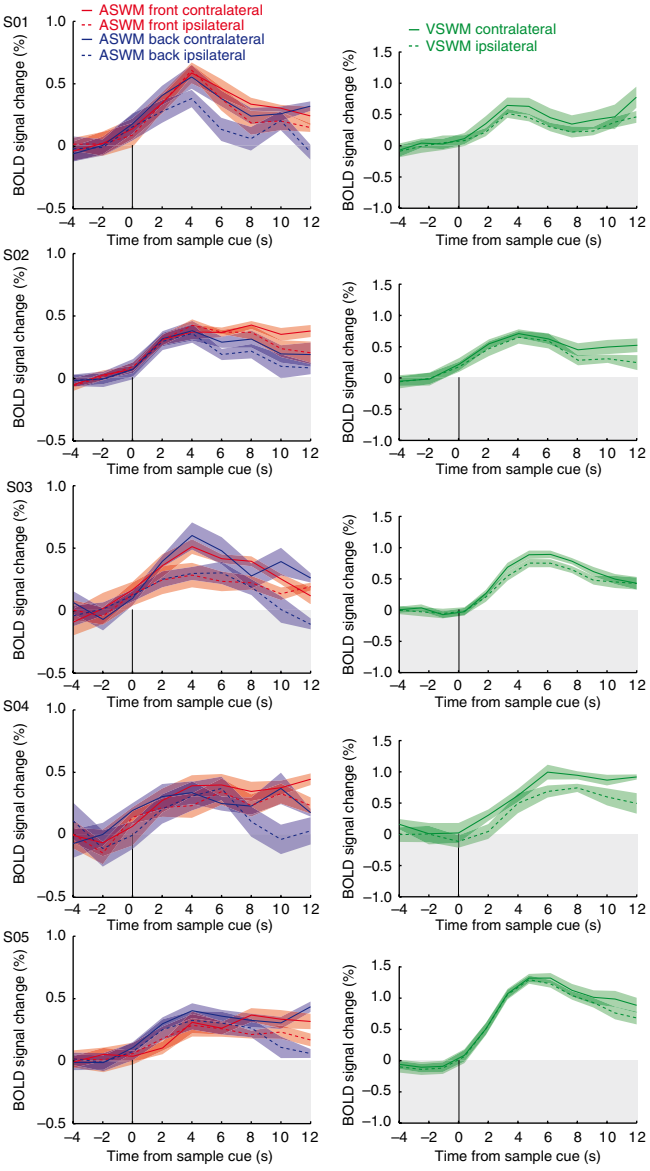

Figure 8 Individual subject BOLD time courses from the sPCS ROI derived from the saccade localizer task. Each time course is time locked to the presentation of the auditory cue (left column) or visual cue (right column), where lines represent the mean signal and band represent s.e.m. ASWM, auditory spatial working memory; VSWM, visual spatial working memory.

the FEF may represent space in a craniotopic, as well as a retinotopic, frame of reference or may represent space in multiple or hybrid frameworks[28,29]. Humans integrate sensory inputs from multiple channels for planning movements in space[30]. The ability to localize sounds may involve the dynamic interplay between spatial representations in head-centered and eye-centered frames of reference that depend critically on the availability and reliability of sensory cues[28,31–35].

In summary, we found persistent activity in the sPCS when maintaining auditory-cued space. The very same area showed overlapping activation during the generation of voluntary saccades and during the maintenance of visually cued space, providing strong evidence that it is the human homolog of the monkey FEF. Because activity persisted even for locations behind the head to which it is impossible to make saccades, activity in the human FEF may also code space in a head-centered, as well as eye-centered, frame of reference.

METHODS

Methods and any associated references are available in the online version of the paper at http://www.nature.com/natureneuroscience/.

Note: Supplementary information is available on the Nature Neuroscience website.

ACKNOWLEDGMENTS

We thank R. Srimal, L. Deouell, S. Inati and K. Sanzenbach for technical support and anonymous reviewers for helpful suggestions. This work was funded by the US National Institutes of Health (R01 EY016407).

AUTHOR CONTRIBUTIONS

K.J.T. and C.E.C. designed and conducted the experiment, analyzed the data and wrote the manuscript.

Published online at http://www.nature.com/natureneuroscience/.
Reprints and permissions information is available online at http://www.nature.com/reprintsandpermissions/.

1. Funahashi, S., Bruce, C.J. & Goldman-Rakic, P.S. Dorsolateral prefrontal lesions and oculomotor delayed-response performance: evidence for mnemonic 'scotomas'. *J. Neurosci.* **13**, 1479–1497 (1993).
2. Curtis, C.E. & D'Esposito, M. The effects of prefrontal lesions on working memory performance and theory. *Cogn. Affect. Behav. Neurosci.* **4**, 528–539 (2004).
3. Rivaud, S., Müri, R.M., Gaymard, B., Vermersch, A.I. & Pierrot-Deseilligny, C. Eye movement disorders after frontal eye field lesions in humans. *Exp. Brain Res.* **102**, 110–120 (1994).
4. Dias, E.C. & Segraves, M.A. Muscimol-induced inactivation of monkey frontal eye field: effects on visually and memory-guided saccades. *J. Neurophysiol.* **81**, 2191–2214 (1999).
5. Ploner, C.J., Rivaud-Pechoux, S., Gaymard, B.M., Agid, Y. & Pierrot-Deseilligny, C. Errors of memory-guided saccades in humans with lesions of the frontal eye field and the dorsolateral prefrontal cortex. *J. Neurophysiol.* **82**, 1086–1090 (1999).
6. Bruce, C.J. & Goldberg, M.E. Primate frontal eye fields. I. Single neurons discharging before saccades. *J. Neurophysiol.* **53**, 603–635 (1985).
7. Funahashi, S., Bruce, C.J. & Goldman-Rakic, P.S. Mnemonic coding of visual space in the monkey's dorsolateral prefrontal cortex. *J. Neurophysiol.* **61**, 331–349 (1989).
8. Chafee, M.V. & Goldman-Rakic, P.S. Matching patterns of activity in primate prefrontal area 8a and parietal area 7ip neurons during a spatial working memory task. *J. Neurophysiol.* **79**, 2919–2940 (1998).
9. Sommer, M.A. & Wurtz, R.H. Frontal eye field sends delay activity related to movement, memory and vision to the superior colliculus. *J. Neurophysiol.* **85**, 1673–1685 (2001).
10. Umeno, M.M. & Goldberg, M.E. Spatial processing in the monkey frontal eye field. II. Memory responses. *J. Neurophysiol.* **86**, 2344–2352 (2001).
11. Curtis, C.E. & D'Esposito, M. Persistent activity in the prefrontal cortex during working memory. *Trends Cogn. Sci.* **7**, 415–423 (2003).
12. Treutwein, B. Adaptive psychophysical procedures. *Vision Res.* **35**, 2503–2522 (1995).
13. Srimal, R. & Curtis, C.E. Persistent neural activity during the maintenance of spatial position in working memory. *Neuroimage* **39**, 455–468 (2008).
14. Curtis, C.E. & D'Esposito, M. Selection and maintenance of saccade goals in the human frontal eye fields. *J. Neurophysiol.* **95**, 3923–3927 (2006).
15. Curtis, C.E., Rao, V.Y. & D'Esposito, M. Maintenance of spatial and motor codes during oculomotor delayed response tasks. *J. Neurosci* **24**, 3944–3952 (2004).
16. Brown, M.R.G. *et al.* Comparison of memory- and visually guided saccades using event-related fMRI. *J. Neurophysiol.* **91**, 873–889 (2004).
17. Russo, G.S. & Bruce, C.J. Frontal eye field activity preceding aurally guided saccades. *J. Neurophysiol.* **71**, 1250–1253 (1994).
18. Kikuchi-Yorioka, Y. & Sawaguchi, T. Parallel visuospatial and audiospatial working memory processes in the monkey dorsolateral prefrontal cortex. *Nat. Neurosci.* **3**, 1075–1076 (2000).
19. Artchakov, D. *et al.* Processing of auditory and visual location information in the monkey prefrontal cortex. *Exp. Brain Res.* **180**, 469–479 (2007).
20. Goldberg, M.E. & Bruce, C.J. Primate frontal eye fields. III. Maintenance of a spatially accurate saccade signal. *J. Neurophysiol.* **64**, 489–508 (1990).
21. Russo, G.S. & Bruce, C.J. Effect of eye position within the orbit on electrically elicited saccadic eye movements: a comparison of the macaque monkey's frontal and supplementary eye fields. *J. Neurophysiol.* **69**, 800–818 (1993).
22. Schall, J.D., Morel, A., King, D.J. & Bullier, J. Topography of visual cortex connections with frontal eye field in macaque: convergence and segregation of processing streams. *J. Neurosci.* **15**, 4464–4487 (1995).
23. Tehovnik, E.J., Sommer, M.A., Chou, I.H., Slocum, W.M. & Schiller, P.H. Eye fields in the frontal lobes of primates. *Brain Res. Brain Res. Rev.* **32**, 413–448 (2000).

24. Chen, L.L. Head movements evoked by electrical stimulation in the frontal eye field of the monkey: evidence for Independent eye and head control. *J. Neurophysiol.* **95**, 3528–3542 (2006).
25. Elsley, J.K., Nagy, B., Cushing, S.L. & Corneil, B.D. Widespread presaccadic recruitment of neck muscles by stimulation of the primate frontal eye fields. *J. Neurophysiol.* **98**, 1333–1354 (2007).
26. Knight, T.A. & Fuchs, A.F. Contribution of the frontal eye field to gaze shifts in the head-unrestrained monkey: effects of microstimulation. *J. Neurophysiol.* **97**, 618–634 (2007).
27. Garg, A., Schwartz, D. & Stevens, A.A. Orienting auditory spatial attention engages frontal eye fields and medial occipital cortex in congenitally blind humans. *Neuropsychologia* **45**, 2307–2321 (2007).
28. Mullette-Gillman, O.A., Cohen, Y.E. & Groh, J.M. Eye-centered, head-centered and complex coding of visual and auditory targets in the intraparietal sulcus. *J. Neurophysiol.* **94**, 2331–2352 (2005).
29. Mullette-Gillman, O.A., Cohen, Y.E. & Groh, J.M. Motor-related signals in the intraparietal cortex encode locations in a hybrid, rather than eye-centered, reference frame. *Cereb. Cortex* **19**, 1761–1775 (2009).
30. Soechting, J.F. & Flanders, M. Moving in three-dimensional space: frames of reference, vectors and coordinate systems. *Annu. Rev. Neurosci.* **15**, 167–191 (1992).
31. Schlack, A., Sterbing-D'Angelo, S.J., Hartung, K., Hoffmann, K.-P. & Bremmer, F. Multisensory space representations in the macaque ventral intraparietal area. *J. Neurosci.* **25**, 4616–4625 (2005).
32. Andersen, R.A. & Zipser, D. The role of the posterior parietal cortex in coordinate transformations for visual-motor integration. *Can. J. Physiol. Pharmacol.* **66**, 488–501 (1988).
33. Mazzoni, P., Bracewell, R.M., Barash, S. & Andersen, R.A. Spatially tuned auditory responses in area LIP of macaques performing delayed memory saccades to acoustic targets. *J. Neurophysiol.* **75**, 1233–1241 (1996).
34. Stricanne, B., Andersen, R.A. & Mazzoni, P. Eye-centered, head-centered and intermediate coding of remembered sound locations in area LIP. *J. Neurophysiol.* **76**, 2071–2076 (1996).
35. Xing, J. & Andersen, R.A. Models of the posterior parietal cortex which perform multimodal integration and represent space in several coordinate frames. *J. Cogn. Neurosci.* **12**, 601–614 (2000).
36. Paus, T. Location and function of the human frontal eye-field: a selective review. *Neuropsychologia* **34**, 475–483 (1996).
37. Ikkai, A. & Curtis, C.E. Cortical activity time locked to the shift and maintenance of spatial attention. *Cereb. Cortex* **18**, 1384–1394 (2008).
38. Curtis, C.E. & Connolly, J.D. Saccade preparation signals in the human frontal and parietal cortices. *J. Neurophysiol.* **99**, 133–145 (2008).

ONLINE METHODS

Subjects. We recruited 13 neurologically healthy individuals (six females, between 22 and 39 years of age) and paid them for their time. All subjects gave written informed consent according to procedures approved by the human subjects Institutional Review Board at New York University.

Auditory spatial working-memory task. The day before scanning, we recorded white-noise bursts (200-ms duration, Polk Audio RM2350 speaker) emitted from 36 locations spaced at 10° increments around every subject's head, seven feet away at ear height, with small microphones placed in their ear canals (KE 4-211-1 microphones, Sennheiser; Firewire 410 MIDI amplifier/digitizer, M-Audio) (**Fig. 1b** and **Supplementary Fig. 3**). Playback of these custom sound recordings via regular stereo headphones preserves the perceived spatial quality of the emitted sounds because the interaural level, timing differences and sound distortions caused by head shadows and ear pinna shape that are specific for each individual are preserved **Supplementary Figures 4–6**. In the scanner, these sounds were presented via MRI-compatible stereo headphones (MR Confon, GmbH) in an auditory spatial working-memory task.

The experimental stimuli were controlled by E-Prime (Psychology Software Tools) and projected (Eiki LCXG100) into the bore of the scanner on a screen that was viewed by the subjects through an angled mirror. We measured BOLD activity while subjects performed 120 trials of the auditory spatial working-memory task (**Fig. 1a**). Each trial began with a preparation cue, either the letter 'F' or 'B' (2 s) that instructed the subject that the sample and test sounds would be coming from in front or behind them. This preparation cue eliminated the occasional confusion that subjects had in pilot testing discriminating front and back space when the cues were close to the midline and interaural timing and level differences are poor spatial clues. After the preparation cue disappeared, the sample sound was presented at pseudo-random locations either in front space or in back space in each trial. Subjects maintained the auditory-cued location over a long and unpredictably variable retention interval (6–14 s). After the delay, a test sound was presented and subjects indicated with a button press of their right index or middle finger whether or not the locations of the sample and test sounds were the same. The sample and test sound locations matched on half of the trials. Match and nonmatch trials were randomly ordered. Subjects were then given feedback ('Correct' or 'Incorrect') followed by an ITI (10–14 s) during which subjects fixated a gray dot allowing the hemodynamic response to return to baseline. Each subject practiced two blocks outside of the scanner on the day before the scanning, and then performed one block of practice in the scanner during the anatomical scans.

The location of the test sound relative to the sample sound on nonmatching trials was determined by the subject's ongoing performance. Notably, as we wanted to compare neural activity during the maintenance of front and back space, we necessarily equated task difficulty across the two conditions for each subject using two independent psychophysical staircases. Task difficulty is a function of the distance between the location of the sample and test sounds (for example, the closer the two sounds are located makes the discrimination more difficult). Separate staircases for front and back space trials kept subjects near a performance threshold of 75% accuracy for both trial types.

Visual spatial working-memory task. Five of the subjects in the auditory spatial working-memory task also participated in a visual version of the task, as described previously[13]. Briefly, each trial began with a preparation cue (a white dot for 2 s) and a sample cue (a cyan square, 150 ms) then appeared at a random location between 5–15° left and right and 4–5° above or below the central fixation. Subjects were asked to maintain the cued location during the following variable delay (6–14 s). After an unpredictable delay, a test cue flashed at or near the sample cue's location (a cyan square for 150 ms) and subjects indicated by a button press whether the two locations matched. Then, subjects were given feedback ('Correct', 'Incorrect') followed by an ITI (10–14 s) during which subjects fixated a gray dot. As with the auditory spatial working-memory task, a staircase procedure was used to determine how close the test cue was presented to the sample cue in non-match trials. Each subject performed 72 visual spatial working-memory trials.

Visually guided saccades. To measure saccade-related activity, we had the same five subjects perform a separate block of 46 trials in which they made saccades to visual targets (a white dot visible for 2 s) that jumped from one position to another randomly (spanning 4–12 degrees of visual angle, ITI 2–12 s). This saccade localizer task was used to define the putative human FEF in the sPCS.

Oculomotor procedures. Because eye movements could confound the ability to test our hypotheses, we instructed subjects to maintain central fixation at all times. All trials in which subjects broke fixation were discarded. Eye position was monitored in the scanner at 60 Hz with an infrared video-graphic camera equipped with a telephoto lens (ASL 504LRO, Applied Sciences Laboratories, custom modified with a Sony HAD CCD) that focused on the right eye viewed from the flat surface mirror mounted inside the radio frequency coil. Because of technical difficulty while recording, two subjects did not have oculomotor data. However, these subjects' eye movements were rated for task compliance by carefully inspecting video recordings of their eye. A total of 97 trials (6.55%) from all subjects were discarded from analyses because of noncompliance.

Neuroimaging methods. We used functional magnetic resonance imaging (fMRI) at 3T (Allegra, Siemens) to measure BOLD changes in cortical activity. During each fMRI scan, a time series of volumes was acquired using a T2*-sensitive echo planar imaging pulse sequence (repetition time, 2,000 ms; echo time, 30 ms; flip angle 80°; 32 slices; 3-mm^3 isotropic voxels; inplane field of view of 192 mm^2; bandwidth, 2,112). Images were acquired using custom radio-frequency coil (NOVA Medical). High-resolution (1-mm^3 isotropic voxels) magnetization-prepared rapid gradient echo three-dimensional T1-weighted scans were acquired for anatomical registration, segmentation and display. To minimize head motion, we stabilized subjects with foam padding around the head.

fMRI data preprocessing and surface-based statistical analysis. *Post hoc* image registration was used to correct for residual head motion (motion correction using FMRIB's Linear Image Registration Tool). We band-pass filtered the time series of each voxel (0.01 to 0.25 Hz) to compensate for the slow drift that is typically seen in fMRI measurements[39,40], divided the time series of each voxel by its mean intensity to convert to percent signal modulation and compensate for the decrease in mean image intensity with distance from the receive coil, and spatially smoothed the data to arrive at a smoothness of 6 mm at full-width half maximum.

For both working-memory tasks, we modeled each within-trial event (that is, sample cue, delay and response) separately, and for the auditory working-memory task, the front and back trial components were separately modeled. The memory delay was modeled by the linear combination of a zero-order polynomial (that is, boxcar) and a first-order polynomial (that is, linear ramp) time-shifted by 4,000 ms to account for the hemodynamic lag. Each of the independent variable regressors were entered into a modified general linear model[41] for statistical analysis using VoxBo (http://www.voxbo.org). We used the first-order polynomial to estimate delay-period activity at the group level because at the individual subject level it predicted significant delay-period activity, which was confirmed by plotting the time courses. In addition, it progressively emphasizes the later portion of the delay, helping decontaminate it from activity evoked during cue processing. For the saccade localizer, we simply modeled the onsets of saccade events.

For each subject, we used Caret (http://brainmap.wustl.edu/caret) for anatomical segmentation, gray-white matter surface generation, flattening and multi-fiducial deformation mapping to the population-averaged landmark- and surface-based atlas[42]. Registering subjects in a surface space using precise anatomical landmark constraints (for example, central sulcus, sylvian and calcarine fissures, etc.) results in greater spatial precision of the alignment compared with standard volumetric-normalization methods[42]. Furthermore, statistical maps for contrasts of interest were created using the beta-weights estimated from each subject's general linear model. These parameter maps were then deformed into the same atlas space and *t* statistics were computed for each contrast across subjects in spherical atlas space. We used a nonparametric statistical approach based on permutation tests to help address the problem of multiple statistical comparisons[43,44], which are even more problematic when one performs statistical analyses on surfaces. First, we constructed a permuted distribution of clusters of neighboring surface nodes with t values > 3.0. We chose a primary t statistic cutoff of 3.0 because it is strict enough that intense focal clusters of activity would pass, but not so strict that diffuse large clusters of activity are lost. In the case of a one-sample comparison, where measured values are compared to the test value

of 0, the signs of the beta values for each node were randomly permuted for each subject's surface, before computing the statistic. One thousand iterations, N, of this procedure were performed to compute a permutation distribution for each statistical test performed. We ranked the resulting suprathreshold clusters by their area. Finally, corrected P values at $\alpha = 0.05$ for each suprathreshold cluster were obtained by comparing their area to the area of the top 5% of the clusters in the permuted distribution, where the critical suprathreshold cluster size, C, at a t score threshold of $t > 3.0$ was $C = N\alpha + 1$. The permutation tests controlled for type I errors by allowing us to formally compute the probability that an activation of a given magnitude could cluster together by chance.

ROI time series procedures. We used ROI-based analyses of the time courses of BOLD signal change. First, on each subject's high-resolution anatomical scans, we traced around gray matter of several a priori ROIs motivated by past studies of visual spatial working memory[13,14,45] and preliminary inspection of single subject activations, including the sPCS, iPL and posterior area of the sTG. Next, in each ROI, we selected the 20 voxels with the strongest main effect of the linear combination of all the task covariates. We plotted the time series of BOLD responses, averaged across voxels in an ROI and averaged across subjects from analogous ROIs, time locked to the presentation of the sample cue, terminating with the last delay volume.

To quantitatively evaluate the time-course data, we created separate cue and delay indices for each ROI. Cue-period activity was defined as the average of the time points in the epoch between 2 and 4 s following the presentation of the sample cue. Delay-period activity was defined as the average of the time points between 6 s following the sample cue until the end of the delay period, which was variable. Additional analyses were performed that restricted the delay period to the end of the delay (that is, the last 10–14 s of the delay period) to help disambiguate the delay period estimates from the cue period estimates. The results from conservative analyses did not differ from the full delay period estimates (see **Supplementary Results 2**).

After confirming that no hemispheric differences existed, we combined data from left and right homologous ROIs. Contralateral activation was defined as activation in the left ROIs when the sample cue fell in the right space, plus activation in the right ROIs when the cue fell in the left space. Ipsilateral activation was defined as activation in the left ROIs to left space cues, plus activation in the right ROI to right space cues. The cue and maintenance indices were plotted against each other with contralateral values on the y axis and ipsilateral values on the x axis and fitted with a linear function. Furthermore, we calculated a laterality index for each subject as the contrast ratio between contralateral and ipsilateral BOLD activity [(contralateral − ipsilateral)/(contralateral + ipsilateral)].

39. Biswal, B.B. & Hyde, J.S. Contour-based registration technique to differentiate between task-activated and head motion-induced signal variations in fMRI. *Magn. Reson. Med.* **38**, 470–476 (1997).
40. Zarahn, E., Aguirre, G. & D'Esposito, M. A trial-based experimental design for fMRI. *Neuroimage* **6**, 122–138 (1997).
41. Worsley, K.J. & Friston, K.J. Analysis of fMRI time-series revisited—again. *Neuroimage* **2**, 173–181 (1995).
42. Van Essen, D.C. Population-average, landmark- and surface-based (PALS) atlas of human cerebral cortex. *Neuroimage* **28**, 635–662 (2005).
43. Holmes, A.P., Blair, R.C., Watson, J.D. & Ford, I. Nonparametric analysis of statistic images from functional mapping experiments. *J. Cereb. Blood Flow Metab.* **16**, 7–22 (1996).
44. Nichols, T.E. & Holmes, A.P. Nonparametric permutation tests for functional neuroimaging: a primer with examples. *Hum. Brain Mapp.* **15**, 1–25 (2002).
45. Curtis, C.E., Rao, V.Y. & D'Esposito, M. Maintenance of spatial and motor codes during oculomotor delayed response tasks. *J. Neurosci.* **24**, 3944–3952 (2004).

doi:10.1038/nn.2406